Geophysical Journal International

Geophys. J. Int. (2021) **224,** 1314–1325
Advance Access publication 2020 October 28
GJI Geomagnetism, rock magnetism and palaeomagnetism

doi: 10.1093/gji/ggaa516

On the distribution of Verwey transition temperatures in natural magnetites

Mike J. Jackson and Bruce Moskowitz

Institute for Rock Magnetism, Department of Earth and Environmental Sciences, University of Minnesota, Minneapolis, MN 55455, *USA.*
E-mail: bmosk@umn.edu

Accepted 2020 October 18. Received 2020 September 29; in original form 2020 June 12

SUMMARY

The Verwey transition in magnetite is a crystallographic phase transition occurring in the temperature range 80–125 K and depends on stoichiometry and cation substitution, which may in turn serve as an indicator of the conditions under which magnetite was formed or altered in nature. We have analysed the distribution of Verwey transition temperatures (T_V) in a large set of samples ($N = 1110$) from a wide variety of rocks, sediments, and other natural and synthetic materials containing magnetite, mined from the database of the Institute for Rock Magnetism and from published studies. The analysis is restricted to measurements of remanence while warming through the transition from which T_V was determined by the derivative method. Our analysis showed that the T_V distribution exhibited a generally bimodal distribution of Verwey transition temperatures, both for the entire data set and for almost all of the lithological subsets. There is a sharp peak for values in the range 118–120 K, and a broad, relatively flat or polymodal distribution from about 98 to 118 K. The upper end of the distribution was sharp, with only a few values exceeding 124 K, and the tail on the lower end extended down to about 80 K. Virtually all of the sample types exhibited polymodal distributions, almost always with one peak near 120 K, and with one or more additional peaks at lower temperatures. Biogenic magnetites produced by magnetotactic bacteria had the lowest modal value of T_V (100 K). Loesses (103.5 K) and igneous extrusives (102.5 K) also had low modal transition temperatures and distributions with dominant low-T_V peaks. Lithological groups with the highest modal transition temperatures were modern soils (119.5 K), silicate minerals with exsolved magnetite (119 K) and sedimentary rocks (119 K). Numerical experiments confirmed that the derivative method for the determination of T_V was reasonably robust and that the observed distributions cannot be explained as an artefact related to the determination of T_V from individual thermomagnetic runs but rather is a general characteristic of natural magnetites. The results provide context for studies that interpret T_V in particular samples in terms of natural processes or conditions during formation or alteration of magnetite.

Key words: Magnetic properties; Environmental magnetism; Magnetic mineralogy and petrology; Rock and mineral magnetism.

1 INTRODUCTION

The Verwey transition is a reorganization of the magnetite crystal structure occurring at a temperature T_V in the range 80–125 K, where the room-temperature cubic inverse-spinel structure transforms to a monoclinic arrangement, and many physical properties of the mineral (e.g. electrical resistivity, heat capacity, magnetic susceptibility, remanence and coercivity) change significantly (e.g. Verwey 1939; Kakol 1990; Shepherd *et al.* 1991; Muxworthy & McClelland 2000; Walz 2002). The temperature of the transition depends strongly on stoichiometry. For pure magnetite (Fe_3O_4), T_V is ∼125 K (Walz 2002), and small amounts of cation deficiency or cation substitution cause significant decreases in T_V, as well as strongly diminishing the changes in physical properties across the transition.

Cation deficiency can originate either by high-temperature (>1000 K) oxidation during initial crystallization and cooling (e.g. Aragon & McCallister 1982; Senderov *et al.* 1993) or by maghemitization at ambient or moderately elevated temperature (e.g. Gallagher *et al.* 1968; Readman & O'Reilly 1971). At high temperature ($T > 1273$ K), a small range of non-stoichiometry ($Fe_{3(1-\delta)}\square_{3\delta}O_4$ with δ not exceeding a few per cent) with vacancy (□) formation is possible depending on oxygen fugacity before crossing over the magnetite–hematite phase boundary (Aragon & McCallister 1982),

and a wide range of cation substitutions are possible (e.g. the titanomagnetite solid solution $Fe_{3-x}Ti_xO_4$ with $0 \leq x \leq 1$). Data from synthetic single-crystal magnetites with controlled high-temperature non-stoichiometry show that T_V decreases progressively with increasing concentration of vacancies or cations, reaching 80 K when x or 3δ approaches 4 per cent (Fig. 1). The rate of shift in T_V from its stoichiometric value is cation dependent and is greatest for Ti^{4+} and Zn^{2+}. A discontinuity in $T_V(x)$ in the data of Honig (1995) at x or $3\delta \sim 0.012$, where the transition temperature drops abruptly from about 110 to 100 K, was interpreted by that author in terms of a change in the transition from first order to second order. This predicts the existence of a gap from about 100 to 110 K, where Verwey transitions do not occur as a result of high-T oxidation or cation substitution. However, the reason why non-stoichiometry or cation substitution abruptly changes the order of the transition is still not known. From all the available data, the transition also ceases to occur for substitutions or vacancy concentrations exceeding about 4 per cent, and we are aware of no reported T_V below about 80 K.

At room temperature or moderately elevated temperatures, magnetite can oxidize to much higher degrees of non-stoichiometry, ultimately to maghemite (γ-Fe_2O_3 with $z \equiv 3\delta = 1/3$). Unlike magnetite, maghemite has no Verwey transition. Intermediate levels of low-temperature oxidation are generally thought to involve core–shell structures with maghemite rims surrounding nearly stoichiometric magnetite cores, and transition zones of high oxidation gradients, through which continued oxidation takes place by diffusion of electrons and vacancies (e.g. Gallagher *et al.* 1968; van Velzen & Dekkers 1999; Özdemir & Dunlop 2010; Chang *et al.* 2013; Almeida *et al.* 2015; Fabian & Shcherbakov 2020). Heating to temperatures above about 150 °C appears to increase the diffusion rate sufficiently to relax the sharp oxidation gradient, relieving stresses associated with the lattice mismatch and resulting in a drop in coercivity (van Velzen & Dekkers 1999). Studies on magnetites that have been experimentally maghemitized to varying extents show that as the overall degree of oxidation increases, the loss of magnetic remanence on warming through the Verwey transition (a) is diminished in magnitude, (b) shifts to lower temperatures and (c) occurs over a broader range of temperatures (e.g. Özdemir *et al.* 1993; Smirnov & Tarduno 2000; Özdemir & Dunlop 2010). As in the case of high-temperature oxidation, vacancy concentrations exceeding about 4 per cent suppress the transition entirely.

The strong sensitivity of T_V to non-stoichiometry has made it difficult to determine whether or not the transition temperature also has an inherent dependence on particle size, especially in the nanometric range, since smaller particles oxidize more easily due to their higher surface/volume ratios. Lee *et al.* (2015) synthesized a set of nanocrystalline magnetite samples with mean particle sizes ranging from 5 to 90 nm, and found a strong apparent size dependence over that interval (Fig. 2). They assert that their nanocrystals are stoichiometric due to the control of fO_2 by appropriate mixing of CO and CO_2 during synthesis. The nanoparticles of magnetite have T_V values still within the range found for single crystal specimens; however, for the smallest sized particles (<10 nm), T_V values fall within the 100–110 K single crystal gap. Other published T_V data for synthetic magnetites of known particle size are uncorrelated with size and are presumably affected by imperfect stoichiometry (Fig. 2).

Other factors that have been shown to affect the transition temperature include applied pressure as well as non-hydrostatic and internal stresses (Rozenberg *et al.* 1996; Carporzen & Gilder 2010; Coe *et al.* 2012; Biało *et al.* 2019). The sensitivity of transition-related magnetic behaviour to factors including particle size, defect density, stoichiometry and stress allows us to make nuanced interpretations of the chemical and physical characteristics of magnetite populations in natural materials, and in some cases to make inferences about their mode of genesis (e.g. Carporzen *et al.* 2006; Carporzen & Gilder 2010; Engelmann *et al.* 2010; Kasama *et al.* 2010; Özdemir & Dunlop 2010; Church *et al.* 2011; Smirnov & Tarduno 2011; Chang *et al.* 2013; Kasama *et al.* 2013; Mang & Kontny 2013; Chang *et al.* 2016).

In this study, the first of its kind, we compile the probability distribution of T_V in a large set of samples comprising a wide variety of rocks, sediments and other natural and synthetic materials containing magnetite. The results provide context for studies that interpret T_V in particular samples in terms of natural processes or conditions during formation or alteration of magnetite. They may also provide insight into the mechanisms of magnetite oxidation in nature.

2 METHODS: DATA MINING AND ANALYSIS

The database of the Institute for Rock Magnetism (IRMDB) contains detailed experimental data from measurements by a few hundred different researchers on a wide variety of materials, with magnetic moment as a function of applied fields, temperature and other variables. Among those data are measurements from a variety of low-temperature experiments, mostly conducted on the IRM's Quantum Designs Magnetic Property Measurement Systems (MPMSs) superconducting quantum interference device (SQUID) magnetometers (MPMS-5S and MPMS-XL), from which T_V can be calculated for samples that contain magnetite, even in quite low concentrations, down to a few ppm.

In principle, one can quantify T_V from measurements of remanence or susceptibility while cooling or warming through the transition, or from more detailed measurements such as hysteresis curves collected as a function of temperature. For consistency, we restrict our analysis to measurements of remanence while warming through the transition, because cooling curves pass through the isotropic point ($T_i \sim 130$ K for $x = 0$) before reaching T_V, and the loss of remanence associated with T_i may be quite large, especially in multidomain magnetites, due to reorganization of domains and the change in magnetocrystalline anisotropy (e.g. Hodych *et al.* 1998; Moskowitz *et al.* 1998; Muxworthy 1999; Özdemir & Dunlop 1999; Liu & Yu 2004; Dunlop 2006), making T_V less clear. The IRMDB software allows interactive analysis and calculation of T_V, as well as the loss of remanence due to warming through the transition, using the derivative method of Liu *et al.* (2004), and more than 1000 values of T_V have been computed and stored by visiting or resident researchers. In a small fraction of the samples where two or more transition temperatures can be identified, more than one T_V has been calculated, but for most samples only a single value has been determined, generally corresponding to the largest derivative peak. In addition to the IRMDB data ($N = 876$), 26 legacy data sets ($N = 234$) from published studies on synthetic and biogenic magnetites and loess are also included in the analysis. The complete data set ($N = 1110$) is provided in the Supporting Information (Tables S1–S3).

Fig. 3 illustrates the analytical approach, which assumes that the loss of remanence on warming is due to the superposition of (1) progressive unblocking over the 20–300 K temperature range [e.g. due to the transition from the stable single-domain (SSD) to the

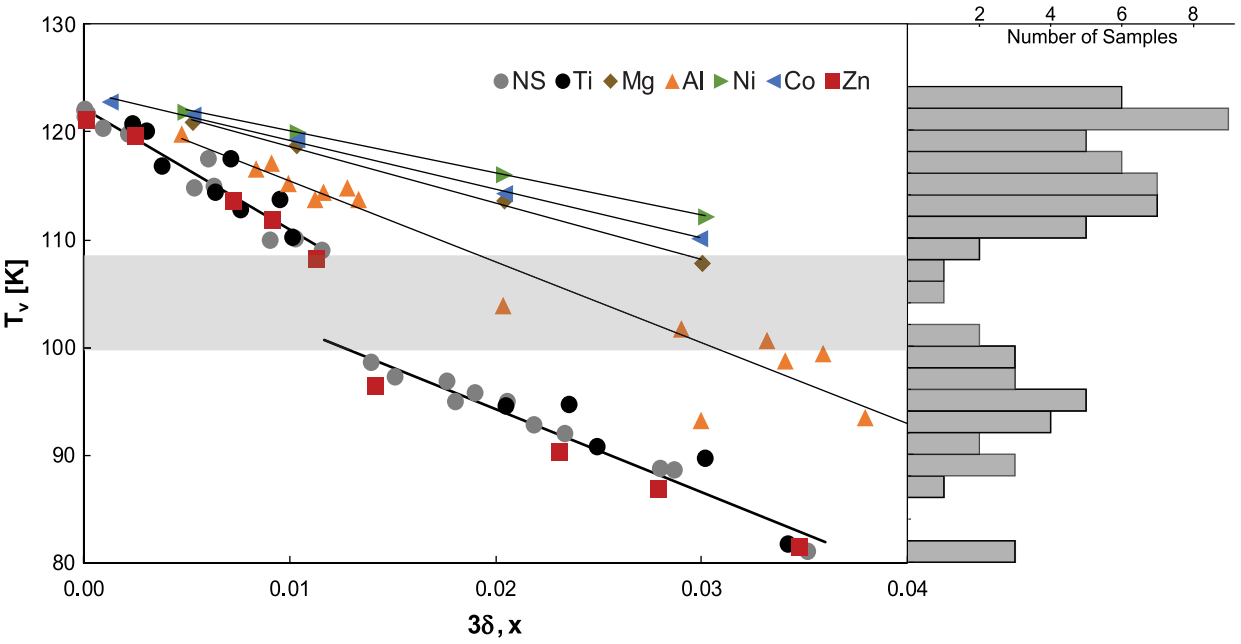

Figure 1. Summary of published data on T_V as a function of non-stoichiometry (δ, NS) and cation substitution with various metals [after Aragón (1992), Honig (1995), Kozlowski *et al.* (1996), Brabers *et al.* (1998), Kakol & Kozlowski (2000) and Švindrych *et al.* (2012)]. Based on magnetic, resistivity and heat capacity measurements on millimetre-sized, single crystals synthesized at high-temperatures ($T > 1273$ K) and controlled oxygen fugacity. Grey box indicates the T_V gap noted by Honig (1995) for NS, Ti and Zn and the marginal distribution is given on the right. Solid lines are best-fit linear trends.

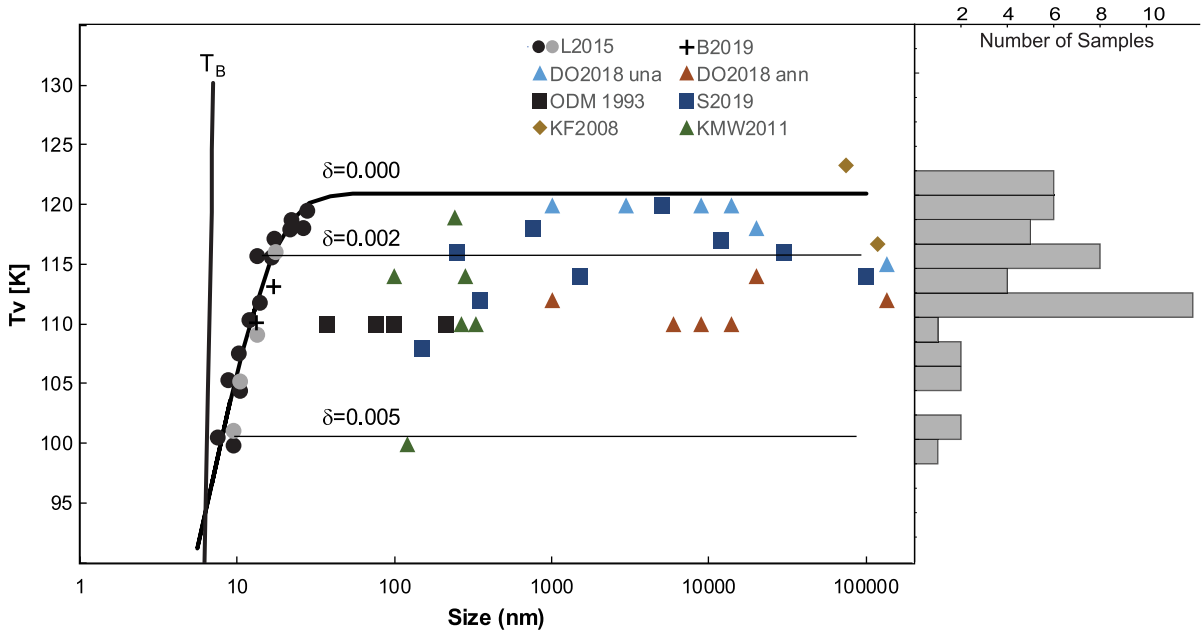

Figure 2. Summary of published data on T_V as a function of particle size (d) and non-stoichiometry (δ). Data for $d < 30$ nm (L2015) are based on electrical conductivity (grey) and magnetization (black), and define the exponential curve shown in black (Lee *et al.* 2015). All other data are based on magnetization measurements. The marginal distribution is given on the right. Nearly vertical grey line represents the size-dependent blocking temperature (T_B) calculated for spherical particles using the anisotropy constant at $T = 4.2$K for the monoclinic phase ($K = 25 \times 10^4$ J m^{-3}, Muxworthy & McClelland 2000). Nanocrystal Verwey transitions are not observed in the superparamagnetic state at temperatures above T_B (i.e. to the left of the black line). Data for $d > 100$ nm include ODM (Özdemir *et al.* 1993); KF2008 (Kosterov & Fabian 2008); S2009 (Smirnov 2009); DO (Dunlop & Özdemir 2018, for annealed (ann) and unannealed (una) samples); B2019 (Barrera *et al.* 2019); KMW2011 (Krása *et al.* 2011) and show significant variation as a function of cation deficiency with no clear trend in grain size. Indicated δ values are based on the data of in Fig. 1.

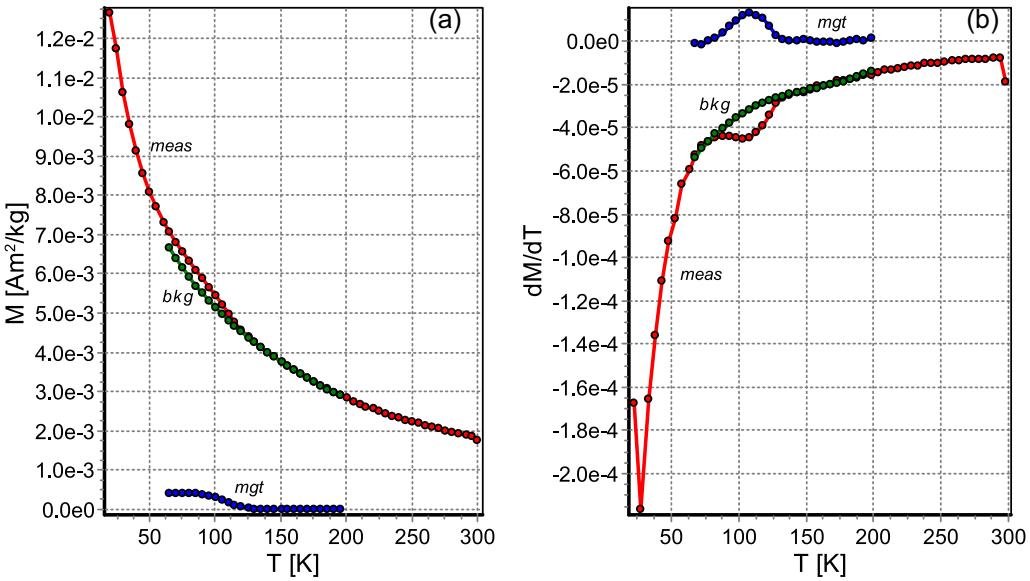

Figure 3. A measured low-T thermal demagnetization curve (a, meas) shows only subtle changes in slope near T_v. The transition is more evident in the derivative curve (b, meas). The 'background' remanence loss due to progressive unblocking of other phases (b, bkg) is approximated by polynomial fitting of specified temperature intervals of the derivative curve, and the difference between the measured and 'background' derivative curves gives the spectrum of remanence loss directly associated with T_v (b, mgt). The integrated background and Verwey-loss derivative curves yield estimates of the isolated demagnetization curves (a).

superparamagnetic (SP) state in nanoparticle populations of magnetite or other magnetic phases] and (2) domain reorganization and intraparticle remanence rotation in a discrete temperature window around T_V, due to the monoclinic-to-cubic transformation in magnetite. In this example the transition is expressed by subtle changes in the slope of the moment-temperature curve (Fig. 3a, red) which become more evident in the derivative curve (Fig. 3b, red). The progressive unblocking is mathematically separated from the discrete remanence loss due to the transition by fitting a low-order polynomial to the derivative curve over a specified temperature range, which spans but excludes the narrower range associated with T_V (e.g. in Fig. 3b, the green curve is a cubic function fit from 65 to 200 K, excluding data between 80 and 135 K). The difference between the polynomial curve and the remanence derivative curve gives the temperature spectrum of the remanence loss due to the transition (blue curve in Fig. 3b), the integral of which is an estimate of the isolated thermal demagnetization curve for magnetite due to the Verwey transition (Fig. 3a, blue curve). The temperature ranges and polynomial order are adjusted interactively by the user to obtain 'reasonable' looking curves for the magnetite demagnetization and the progressive unblocking (i.e. curves that are monotonic, and fits that are within the measurement noise, while minimizing the polynomial degree). The value of T_V is calculated as the location of the peak of the T_V spectrum, determined as the interpolated zero crossing of the derivative of the spectrum curve.

The accuracy of the transition temperatures determined in this way depends on several factors including thermal lag, the accuracy of the individual temperature measurements, any systematic differences between the two MPMS magnetometers, the temperature increment, the signal/noise ratio and the symmetry or asymmetry of the T_V spectrum. First, thermal lag may result in an apparent offset of T_V, related to the temperature sweep rate and the specimen mass (thermal inertia). The warming rate for the vast majority of experimental runs was 5 K min^{-1} (a *de facto* standard laboratory protocol, which renders any thermal lag insignificant for most samples). Because the heating rate was the same in most runs, and specimen volumes and masses were strongly constrained by instrument geometry, we are confident that these factors did not significantly shape the observed T_V distributions. Second, the temperature measurement accuracy of the two MPMS magnetometers (MPMS-5S and MPMS-XL) and any systematic differences between the two was addressed by comparing results from the magnetometers. Queries in the database were run to compare measurements between the two instruments (a) for individual specimens that had been run in both of them and (b) for the full sample set. The first of these comparisons addressed the question most directly, since the T_Vs obtained for an individual specimen should be identical for both instruments. The number of these was relatively small, so the overall distribution for the full sample set obtained from each instrument was also compared. In both instances, we found no indication of systematic differences between the two instruments.

We have evaluated the remaining factors by numerical experimentation, constructing synthetic thermal demagnetization curves with Gaussian spectra having specified means and standard deviations, and adding random noise with specified ranges of magnitude. These synthetic data sets were processed in the same way as the measured data, and errors were calculated as the difference between specified and calculated T_V. Details of the numerical procedures are provided in the Supporting Information (Text S1) and summarized in Section 3.2.

3 RESULTS

3.1 Observed distribution of T_V across the sample set and lithology

Fig. 4 shows the frequency distribution, in 2° bins, of observed T_V values for the full data set of 1110 low-temperature measurements. It also shows a smoothed curve as an estimate of the underlying probability distribution, as well as two best-fit models (which will

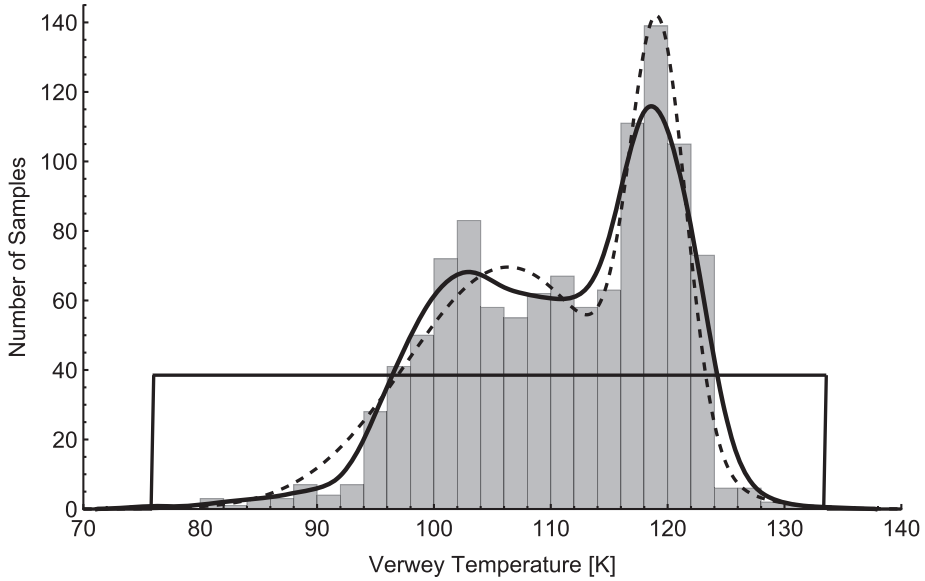

Figure 4. Probability distribution of Verwey transition temperatures. Data from (1) the IRM database, computed from low-temperature remanence measurements by IRM facility users on a wide variety of natural materials and synthetic analogues and (2) published data. The data set includes Verwey transition temperatures determined from magnetic ($n = 1042$), electrical resistivity ($n = 38$) and heat capacity ($n = 30$) experiments. See the Supporting Information for data sources. Solid curves are smoothed approximation of probability density function and best-fit uniform distribution ($p < 0.001$). Dashed curve is best-fit multicomponent distribution composed of two Gaussian distributions ($p = 0.243$).

Table 1. Modal Verwey transition (T_V) temperatures for broad categories of natural and synthetic magnetites.

Material	*N*	Modal T_v1 (K)	Modal T_v2 (K)
Biogenic(bm)	82	100	115.5
Dust	53	117.5	104.5
Extraterrestrial(et)	4	121.5	—
Loess/palaeosol	67	103.5	120
Metamorphic rock(mr)	44	116.5	99.5
Silicate crystals(ssc)	15	119	108
Sediment (unlithified, sed)	127	118.5	99
Soil	106	119.5	105.5
Sedimentary rock (sr)	109	119	102
Synthetic powders (smp)	101	109	117.5
Synthetic single crystals (scm)	75	117	94,5
Igneous extrusive (ext)	126	102.5	110.5
Igneous intrusive (int)	121	119,5	103.5
Non-classified (nc)	80	108.5	102
All data	1110	118.5	103

Modal T_v1 and Modal T_v2 values correspond to the largest and second largest peak in transition temperature distribution. Samples that could not be easily grouped into lithological subsets are designated as non-classified.

be described in more detail in Section 3.3): (a) a uniform probability distribution and (b) a multicomponent model 'unmixed' in Mathematica, where each component may be Gaussian, log-Gaussian or uniform, and in which the number of components is the minimum determined by the algorithm to be necessary for a statistically acceptable fit. There is a sharp peak for values in the range 118–120 K, and a broad, relatively flat or polymodal distribution from about 98 to 118 K. The upper end of the distribution is sharp, with only a few values exceeding 124 K, and the tail on the lower end extends down to about 80 K.

We have classified the sample types for these measurements into broad categories (Table 1) and isolated the T_V distribution for each type (Figs 5a and b). Virtually all of the sample types exhibit polymodal distributions, almost always with one peak near 120 K, and with one or more additional peaks or plateaus at lower *T*. The biogenic magnetites have a very weak 120 K peak, and they have the lowest modal T_V, 100 K. Loesses (103.5 K) and igneous extrusives (102.5 K) also have relatively low modal transition temperatures and distributions with dominant low-T_V peaks, presumably because they are relatively oxidized or contain minor cation substitutions. Interestingly, however, the loess distribution has a sharp lower bound just below 100 K. The groups with the highest modal transition temperatures are the soils (119.5 K), silicate minerals with exsolved magnetite (119 K) and sedimentary rocks (119 K). Although most of the lithologic subsets exhibit bimodal or multimodal distributions, the gap observed by Honig (1995) between 100 and 110 K [seen in Fig. 1 and the single-crystal magnetite (scm) binned frequency plot in Fig. 5b] for high-temperature non-stoichiometry is not clear in our data.

3.2 Resolution and accuracy of T_V determinations

In order to properly understand these results, it is important to consider whether the method of estimating T_V for individual specimens may introduce some bias or artefacts into the observed distributions. In the supplementary material, the numerical experiments demonstrate the following. First, when the isolated low-*T* demagnetization derivative curves (e.g. Fig. 3b) are unimodal and reasonably symmetric (i.e. when there is a single dominant T_V with the remanence loss spread over an interval centred on T_V), random measurement noise may shift individual estimates to higher or lower *T,* but there is no systematic bias in any sufficiently large set of such determinations. Similarly, if there are two distinct transition temperatures in the data for a specimen, and the individual derivative peaks are adequately separated due to narrow distributions and/or large temperature differences, the larger peak is reliably quantified, provided noise is not excessive, and again there is no systematic bias in the estimates. Because the method determines the temperature at which the derivative is maximum, the 'larger peak' is not necessarily the

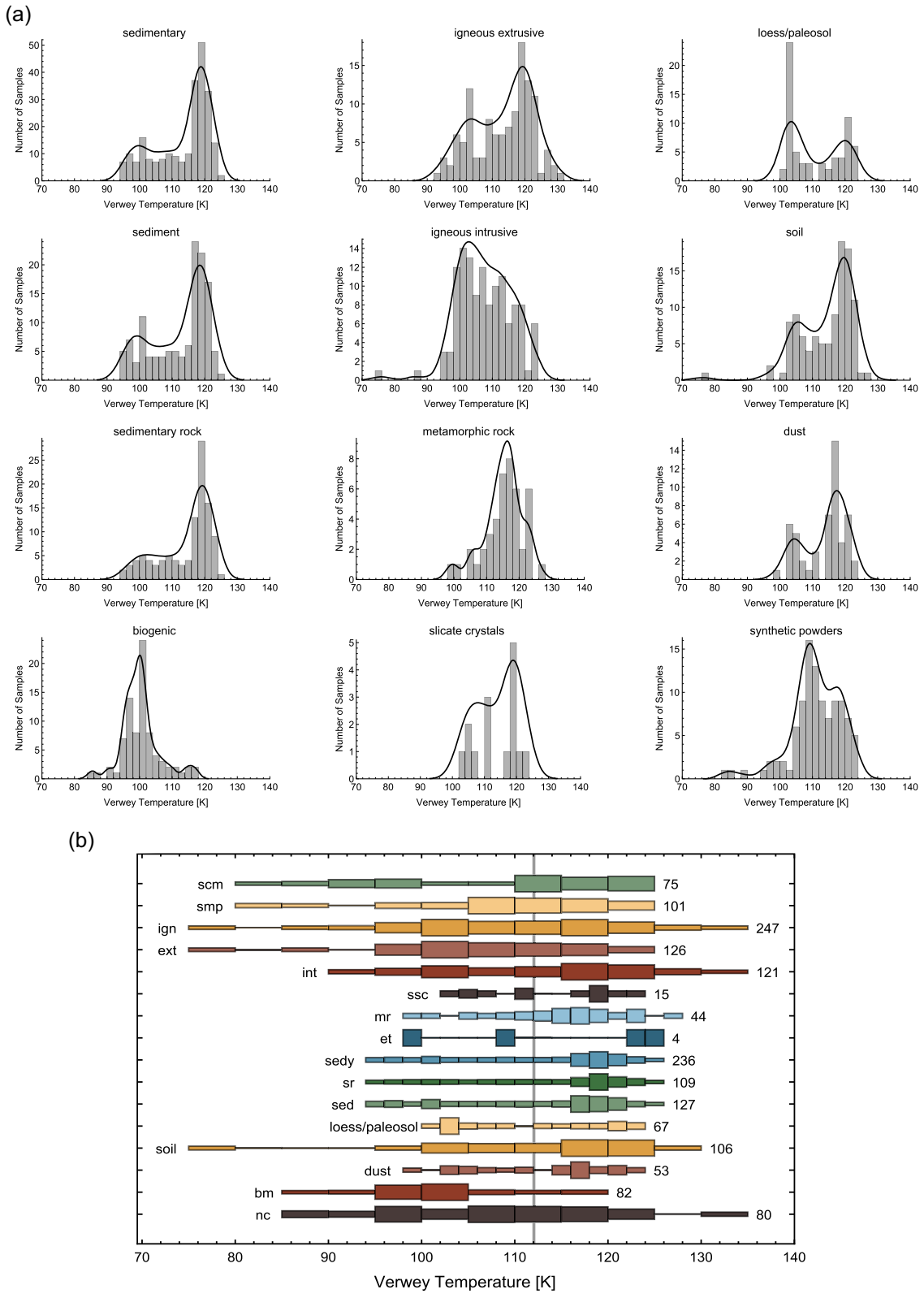

Figure 5. (a) Probability distribution of Verwey transition temperatures grouped by type of material: sediments—unlithified sediment (other than loess/soil); sedimentary rock; sedimentary—combined sediments and sedimentary rock; biogenic—intracellular biogenic magnetite. Curves are smoothed probability density function approximations. (b) Binned frequency plot of Verwey transition temperatures grouped by type of material: scm—single-crystal magnetite (synthetic); ign—combined igneous intrusive(int) and extrusive(ext); sed—unlithified sediment (other than loess and soil); sr—sedimentary rock; sedy—combined sed and sr; nc—not classified; et—extraterrestrial; scc—silicate minerals with exsolved magnetite; smp—synthetic magnetite powders; mr—metamorphic rock; bm—biogenic magnetite. Grey vertical line is median T_v value for all data and numbers on the right indicate total number of T_v values in each sample set. The scm data set are single-crystal magnetites synthetized at high temperatures (see Fig. 1).

one associated with the largest loss of remanence (area under the derivative peak).

When there are two or more populations of magnetites in a sample, with different T_Vs and strongly overlapping derivative spectra, the derivative peak may not coincide with any of the individual component T_Vs, and in this way some bias may be introduced. For example, two populations with individual Gaussian T_V spectra having significantly overlapping peaks of equal height and equal width will, even in the absence of measurement noise, yield an estimate of T_V that is the average of the two component T_Vs. However, we have found no scenario by which measurement noise, sampling interval, or other factors, produce a spurious bimodal or multimodal distribution of apparent T_Vs from an underlying unimodal T_V spectrum. Thus the bi/multimodality of the observed T_V distributions can be considered a robust result.

3.3 Statistical significance of the observed bimodality

The observed distributions generally appear to be convincingly bimodal under visual inspection, but it is preferable to estimate the significance of this in a quantitative way. Statistical tests for bimodality are complicated due to the unknown nature of the underlying unimodal distributions, and are sensitive to factors including whether the underlying distributions are Gaussian, how much they are skewed, and how much their peaks are separated compared to their widths (e.g. Jackson *et al.* 1989; Frankland & Zumbo 2002, 2009). Nevertheless, it is important to demonstrate that the observed distributions have some statistical significance, and that they would be very unlikely to arise, for example, by random sampling from a uniform probability distribution (i.e. a null hypothesis that T_Vs in natural materials are equally likely to have any value between, say 80 and 125 K). The black curve in Fig. 4 shows a uniform distribution fit over the full range of measured values; it is obviously a poor fit to our data, and the calculated probability that the observed data set could have arisen by random sampling from such a distribution is vanishingly small ($p < 0.001$).

However that test does not address the question of whether or not the observed distribution is truly multimodal or merely non-uniformly distributed (e.g. a unimodal Gaussian distribution would also fail the uniformity test). In order to obtain an approximate measure of the significance of the apparent bimodality, we can formulate another simple test based on the null hypothesis that Verwey transition temperatures in natural materials have a uniform probability distribution between, say, 100 and 124 K (excluding the tails of the observed distribution for this test). If we divide this temperature range into 3 equal intervals (100–108, 108–116 and 116–124), we would expect each interval to contain about 1/3 of all of the measured T_Vs under the null hypothesis ($p_0 = 1/3$). Counts much higher or lower than that would argue against the observed values being random draws from a uniform pdf.

For N total samples, the probability of observing n values in any of the intervals is given by the binomial distribution. In our data set, 945 of the values lie in the interval [100, 124], and thus about 315 would be expected in each bin for random draws from a uniform probability distribution ($<n> = 315$). As shown in Table 2, the low and intermediate T_V ranges contain many fewer samples than expected under the null hypothesis, and the high T_V range contains many more. Because of the large value of N, the binomial probability density function (bpdf) is quite narrowly peaked, and counts n deviating so strongly from $<n>$ are extremely unlikely to arise by chance. The low T_V range contains just 268 of the 945 samples. The

Table 2. Bimodal significance test.

Range	Midpoint	Count	bcpf	1-bcpf
100–108	104	268	5.80E-04	
108–116	112	250	2.88E-06	
116–124	120	427		1.64E-14
	total N	945		

bcpf, binomial cumulative probability function.

binomial cumulative probability function (bcpf) indicates that the probability of observing a bin count of 268 or lower out of 945 samples is 5.8×10^{-4} and thus it is clear that the null hypothesis must be rejected. For the intermediate and high T_V ranges, the counts deviate even more strongly from $<n>$. The bcpf indicates a probability of only 2.9×10^{-4} for observing a count of 250 or lower, as seen for the intermediate range, and (1–bcpf) indicates a probability of only 1.6×10^{-14} for observing a count of 427 or higher, as seen for the high T_V range. Thus the possibility of the observations arising from random sampling of a uniform probability distribution is resoundingly rejected, but moreover, for the full data set the high-T_V range is significantly overrepresented, while the low range and especially the intermediate range are significantly underrepresented, supporting the assertion that the distribution is multimodal. We can repeat the analysis for the two lower-T intervals alone (100–116 K, $N = 518$, $<n> = 259$) to evaluate the statistical significance of the different bin counts representing the lower-T peak and intermediate-T range of low occurrence ($n_1 = 268$, $n_2 = 250$). The probability of obtaining counts as high or as low as those by random draws from a uniform probability distribution are respectively about 20 per cent and 23 per cent, i.e. unlikely but with rather low statistical significance.

Finally, we used the Mathematica routine, FindDistribution, for unmixing the observed T_V distributions into sums of component Gaussian, log-normal and uniform distributions. This routine automatically finds the simplest set (minimum number) of components that provides a statistically acceptable fit to a set of observations. For the full data set (Fig. 4), and for all but four of the lithological subsets, two or more components were required for an acceptable fit (Supporting Information Figs S7 and S8).

4 DISCUSSION

A number of studies over the last 15 yr have noted the co-occurrence of two distinct T_Vs in individual specimens of a variety of materials (e.g. Liu *et al.* 2004; Carporzen *et al.* 2006; Mang & Kontny 2013; Carlut *et al.* 2015; Chang *et al.* 2016; Longchamp 2019). In such specimens, as well as in the large collections of specimens in this study, the co-occurrence of distinct T_Vs immediately suggests the coexistence of distinct populations of magnetite grains with different stoichiometries, cation substitutions, or perhaps different defect densities and internal stresses. Recognition of the occurrence of these populations may lead to significant insights into the nature of the material and the processes that have affected it.

Bimodal T_V distributions observed in individual specimens have been interpreted in previous work in terms of material properties and conditions of formation/alteration: (a) in Chinese loess/palaeosol samples, Liu *et al.* (2004) attributed low and high T_Vs (~108 and 120 K) respectively to fine (oxidized) pedogenic and coarser detrital magnetite fractions; (b) in the Vredefort structure, Carporzen

et al. (2006) interpreted SD-PSD grains that crystallized during impact as the sources of an observed low T_V (100 K), while a high T_V (125 K) was associated with PSD-MD grains that formed in the pre-shock basement; (c) in the Chesapeake Bay impact structure, Mang & Kontny (2013) found both low and high T_Vs (∼92 and 122 K) associated with large unshocked MD grains and with highly shocked magnetites with reduced grain sizes, whereas only low T_Vs were found in secondary magnetites formed during or after the impact; (d) in Archean Banded Iron Formation samples from Western Australia, Carlut *et al.* (2015) found a 120–124 K transition which they attributed to nearly pure stoichiometric magnetite, and one around 105–110 K, which SEM and microprobe observations suggested was related to microbial-induced partial substitution of iron by silicon; (e) in continental-margin marine sediments for which FORC data and SEM observations indicated the presence of significant populations of intact magnetosome chains produced by magnetotactic bacteria (MTB), Chang *et al.* (2016) observed two prominent T_V values (near 100 and 120 K), which they attributed to magnetites of respectively biogenic and inorganic origin; and (f) in pseudo-tachylytes from the South Mountains, Arizona (*Longchamp* 2019), a low T_V (105 K) and an extraordinarily high T_V (128 K) are respectively associated with SD and MD particles, as indicated by the relative magnitudes of field-cooled and zero-field-cooled remanences (Kosterov 2003; Carter-Stiglitz *et al.* 2006); the finer particles with lower T_V are considered to be neoformed magnetite grains that crystallized during rapid melt quenching.

Thus, the coexistence of populations with differing stoichiometries suggests different processes or conditions of magnetite formation or alteration, the details of which depend on the geologic context. Although in several cases the populations are inferred to have different average particle sizes and domain states, the relation between T_V and size is indirect; that is, the reduction in T_V is not caused by finer particle size, but rather by higher non-stoichiometry in the finer population, which is interpreted to have formed under different conditions.

In the large groups of samples of this study, the bimodality of the T_V distribution is most conspicuous for the sediments (including dust, loesses, soils, other sediments and sedimentary rocks), with well-defined peaks near 100 and 120 K, and a distinct minimum near 110 K. Among these sedimentary groups, all except the loesses have a dominant peak at 120 K and a subordinate one at 100; for the loesses the reverse is true. Loesses are generally considered to contain relatively unweathered detrital magnetites, whereas the magnetite in soils is commonly thought to be a mix of more strongly weathered detrital grains and pedogenic particles formed *in situ* (Maher & Thompson 1999; Evans & Heller 2003; Liu *et al.* 2012). The bimodality observed for dust samples, which come from filter and dust-on-snow sampling (Reynolds *et al.* 2014a,b, 2020), may represent mixtures of magnetite from natural and anthropogenic sources whose properties would be highly site dependent.

The T_V bimodality in the other sedimentary groups (dust, non-aeolian sediments and sedimentary rocks) may also in many cases have a straightforward explanation. Chang *et al.* (2016) propose that the occurrence of two distinct T_V temperatures in marine and lake sediments is a diagnostic signature for the co-occurrence of biogenic and inorganic magnetite. Our compilation confirms that MTB magnetosome chains generally have relatively low T_V, commonly around 100 K (Fig. 6), as has been noted previously even for freshly cultured cells (e.g. Moskowitz *et al.* 1993; Kopp *et al.* 2006a, b; Moskowitz *et al.* 2008; Li *et al.* 2012; Chang *et al.* 2016). The reason for this remains unclear. X-ray magnetic circular dichroism (XMCD) studies (Coker *et al.* 2007; Lam *et al.* 2010) found that intracellular nano-magnetite in magnetotactic bacteria had ferrous/ferric cation site occupancy ratios close to that of stoichiometric magnetite, with a slight excess of ferrous iron. In a variable-temperature Mössbauer study on wet-packed cells of MS1 (*Magnetospirillum magnetotacticum*), Frankel *et al.* (1983) reported that spectra taken at 200 K indicated some surface oxidation of magnetosomes and that T_V occurred between 110 and 130 K. Nevertheless, given the common occurrence of T_V ∼100 K in nearly all of the material classes of this study, it must be conceded that any relatively low T_V occurring in sediments may have sources other than MTB, and the inference that a biogenic magnetite population is present has some uncertainty attached.

There is an important and heretofore underappreciated caveat to these interpretations, which we wish to emphasize here: the observed bimodality of transition temperatures in these data sets does not necessarily require a corresponding bimodality of composition, because of the possible existence of a discontinuity in $T_V(x)$. In the original study of Honig (1995), the superposition of the trends for $T_V(x_{Ti})$, $T_V(x_{Zn})$ and $T_V(3\delta)$ (Fig. 1) suggested a universal dependence of the transition temperature upon limited cation substitution and non-stoichiometry, which would in principle allow estimation of the deviation from pure Fe_3O_4 composition by using measured T_V values. Such an estimation would produce a relatively compressed distribution of x values, necessarily narrower than the distribution of T_V values because of the discontinuity in $T_V(x)$. The apparent universality of $T_V(x)$ was subsequently disproven by additional data from magnetites doped with Al, Co, Ni and Mg (Fig. 1); Kakol *et al.* (2012) suggest the different trends may be related to the fact that these ions substitute into both the A and B sites, in contrast to Ti and vacancies (which enter only into B sites) and Zn (which strongly prefers A sites). In any case, using measured T_V values to estimate composition would at best be very complicated due to the different trends for different substituents (Fig. 1). Nevertheless, it remains true that the distributions of composition may very well be narrower than those observed for T_V, and may even be unimodal in some cases.

How then, can we determine the true significance of an observed bimodality of T_V, in an individual specimen or in a large group of specimens? Unfortunately, there are various complicating factors and we are unable to give a simple and universally applicable answer. One complication is the fact that the 'Honig gap' (the temperature interval for which T_Vs are not expected to occur based on high-T non-stoichiometry experiments, [100,108]), does not exactly correspond with the intermediate interval in which the observed frequency of occurrence is relatively low in our data set (approximately [104,116]). This suggests that T_Vs in natural magnetites may be affected by mechanisms not represented in those experiments. For example, natural magnetites may contain several different cations and their combined effects may produce T_V values within the Honig gap. Another important consideration is that whereas the high-temperature cation-deficient magnetites are homogeneous in composition, natural partially oxidized magnetites are distinctly heterogeneous, with strongly oxidized outer shells surrounding more stoichiometric cores, and strong intraparticle chemical gradients. A $T_V(z)$ calibration based on high-T homogeneous oxidation would suggest that each particle of magnetite that is partially oxidized at ambient T would have a spectrum of transition temperatures and a corresponding spectrum of remanence loss while heating; however that is at or beyond the limits of what can be observed experimen-

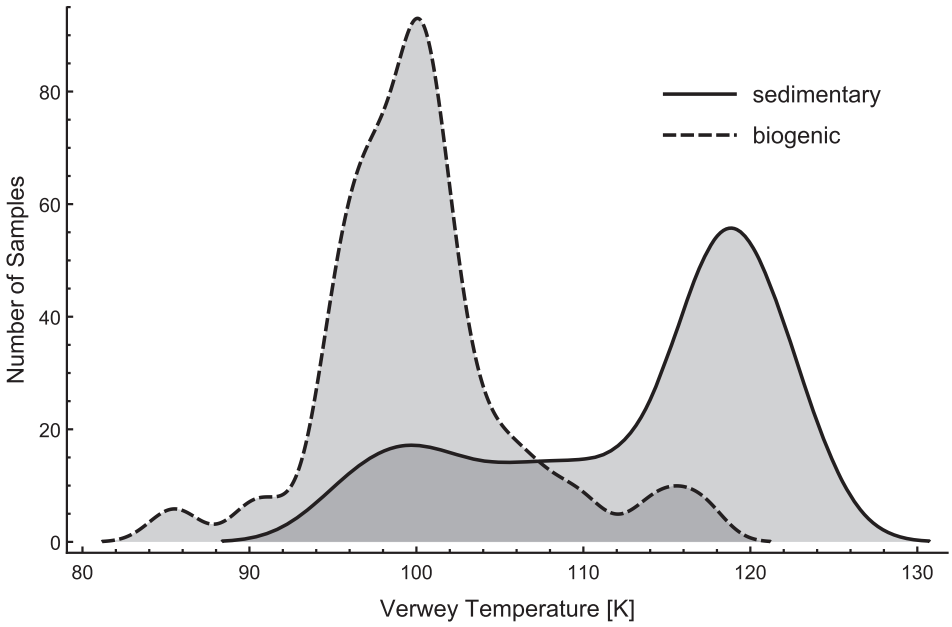

Figure 6. Comparison of Verwey temperatures determined for biogenic magnetites produced by magnetotactic bacteria (dashed line) and for all other sedimentary magnetites (solid line). Curves are smoothed probability density function approximations.

tally or simulated micromagnetically. We believe it is still likely that the observed T_V distributions generally contain significant information on magnetite compositions and on the natural processes that have influenced them, but interpretations are neither unique nor universal. The possible existence of a gap in $T_V(x)$ may increase the sensitivity with which we can detect small changes in composition, magnifying them into larger differences in T_V. On the other hand, the difficulty of distinguishing individual peaks in demagnetization spectra of samples with strongly overlapping components means that many of the T_V values obtained may represent weighted averages of those of the unresolved individual components.

The magnetites that formed in-situ at ambient temperatures, by pedogenesis and by MTB, generally contain no cations of other metals substituting for Fe, and therefore cation deficiency is the only form of non-stoichiometry in them. In contrast, for the low-T_V magnetites formed in-situ at high temperatures in meteorite impacts and in pseudo-tachylytes in earthquake fault zones, cation substitution may be more common (in part as a result of the large number of different cations that the spinel structure can accommodate at high temperatures in igneous systems). Thus there are at least two ways to account for the frequent occurrence of low T_Vs in non-sedimentary materials.

It is appropriate to wonder whether some of the accumulated T_Vs in our data set may in fact be attributable to other types of critical temperature that have been incorrectly interpreted as the magnetite transition. Accelerated remanence loss over discrete temperature intervals in a similar range may also be produced in titanomagnetites of particular compositions, by other mechanisms including isotropic points (where the first magnetocrystalline anisotropy constant changes sign) (e.g. Kakol *et al.* 1991; Moskowitz *et al.* 1998; Engelmann *et al.* 2010) and 'pinning transitions' (related to thermally activated electron hopping and magnetoelastic wall pinning in titanomagnetites, *Church et al.* 2011). Additionally there are other magnetic mineral systems that have ordering temperatures within the range of our tabulated T_Vs, including chromites ($FeCr_2O_4$) (e.g. Klemme *et al.* 2000; Antretter *et al.* 2003; Gattacceca *et al.* 2011), which could potentially be misidentified as Verwey transitions. Although some small fraction of our tabulated T_Vs may be mistakenly identified as such, we consider it very unlikely that the number is significant enough to have a discernible effect on the T_V distributions that we have compiled, because of the limited range of compositions involved and the general rarity of those compositions in natural materials.

The derivative method that we have employed for determination of T_V is reasonably robust but in some cases with multiple transition temperatures and strongly overlapping ranges, the method yields a temperature that may not accurately reflect any of the component populations. For proper identification of coexisting T_Vs in a single sample, it is preferable to unmix the temperature spectra in the same way that coercivity spectra are analysed, and similar to the methods we have used for the large sets of samples in Fig. 4 and in the Supporting Information. Reanalysis of the individual demagnetization curves for the large sample set, however, is beyond the scope of this study.

5 SUMMARY AND CONCLUSIONS

A large sample set, containing a wide variety of lithologies as well as synthetic magnetites and cultured magnetotactic bacteria, exhibits a generally bimodal distribution of Verwey transition temperatures, both for the set as a whole and for almost all of the lithological subsets. The observed distribution cannot be explained as an artefact related to the methods involved in the determination of T_V for individual thermomagnetic runs, and we consider it to be a general characteristic of natural magnetites. Published data on synthetic magnetites with controlled cation substitutions or cation deficiency show discontinuities at critical compositions that are thought to represent a change from first-order to second-order transitions, resulting in gaps in the distribution of transition temperatures for

those samples. Therefore, our observed broad and bimodal distributions of T_V may not necessarily correspond to equally broad or bimodal distributions of magnetite composition. Nevertheless, the transition temperature is a sensitive indicator of magnetite purity, which may in turn serve as an indicator of the conditions under which the magnetite formed or was altered.

A significant number of studies have documented the occurrence of double Verwey transitions in individual samples, and have suggested plausible interpretations involving distinct populations of magnetite produced by context-specific mechanisms. We endorse this approach, and extend it to larger sample groups, in which each sample exhibits a single well-defined T_V while the whole population displays a broad and multimodal distribution of transition temperatures. However we caution against viewing any specific interpretation as universally applicable as (1) the distribution of magnetite compositions may be significantly more compact than that of transition temperatures, due to the possibility of a gap in $T_V(x)$ and (2) a broad and bimodal or multimodal distribution of T_V appears to be a common feature of almost all natural materials containing magnetite.

ACKNOWLEDGEMENTS

We are grateful to the many talented scientists who have used the IRM instrumental facilities for their research and uploaded data to the IRMDB, some of the results of which we have used in this study. We thank reviewers Karl Fabian and Adrian Muxworthy for their insights and helpful suggestions. This research was made possible by support for the Institute for Rock Magnetism by the NSF Division of Earth Sciences, Instruments and Facilities program, and by the University of Minnesota. This is IRM contribution #2003. All data used in this paper are included in the Supporting Information.

REFERENCES

Almeida, T.P., Muxworthy, A.R., Kasama, T., Williams, W., Damsgaard, C., Frandsen, C., Pennycook, T.J. & Dunin-Borkowski, R.E., 2015. Effect of maghemization on the magnetic properties of nonstoichiometric pseudo-single-domain magnetite particles, *Geochem. Geophys. Geosyst.,* **16**(9), 2969–2979.

Antretter, M., Fuller, M., Scott, E., Jackson, M., Moskowitz, B. & Solheid, P., 2003. The paleomagnetic record and rock magnetism of Martian meteorite ALH84001, *J. geophys. Res.,* **108**(E6), doi:10.1029/2002JE001979.

Aragón, R., 1992. Magnetization and exchange in nonstoichiometric magnetite, *Phys. Rev. B* **46**(9), 5328–5333.

Aragón, R. & McCallister, R.H., 1982. Phase and point defect equilibria in the titanomagnetite solid solution, *Phys. Chem. Miner.,* **8**(3), 112–120.

Barrera, G., Tiberto, P., Sciancalepore, C., Messori, M., Bondioli, F. & Allia, P., 2019. Verwey transition temperature distribution in magnetic nanocomposites containing polydisperse magnetite nanoparticles, *J. Mater. Sci.,* **54,** 8346–8360.

Biało, I. *et al.*, 2019. The influence of strain on the Verwey transition as a function of dopant concentration: towards a geobarometer for magnetite-bearing rocks, *Geophys. J. Int.,* **219**(1), 148–158.

Brabers, V.A.M., Walz, F. & Kronmüller, H., 1998. Impurity effects upon the Verwey transition in magnetite, *Phys. Rev. B,* **58**(21), 14163–14166.

Carlut, J. *et al.*, 2015. Low temperature magnetic properties of the Late Archean Boolgeeda iron formation (Hamersley Group, Western Australia): environmental implications, *Front. Earth Sci.,* **3**(18), doi: 10.3389/feart.2015.00018.

Carporzen, L. & Gilder, S.A., 2010. Strain memory of the Verwey transition, *J. geophys. Res.,* **115**(B5), B05103, doi: 10.1029/2009jb006813.

Carporzen, L., Gilder, S.A. & Hart, R.J., 2006. Origin and implications of two Verwey transitions in the basement rocks of the Vredefort meteorite crater, South Africa, *Earth planet. Sci. Lett.,* **251**(3-4), 305–317.

Carter-Stiglitz, B., Moskowitz, B., Solheid, P., Berquo, T.S., Jackson, M. & Kosterov, A., 2006. Low-temperature magnetic behavior of multidomain titanomagnetites: TM0, TM16, and TM35, *J. geophys. Res.,* **111,** B12S05, doi:10.1029/2006JB004561.

Chang, L. *et al.*, 2013. Low-temperature magnetic properties of pelagic carbonates: oxidation of biogenic magnetite and identification of magnetosome chains, *J. geophys. Res.,* **118**(12), 6049–6065.

Chang, L., Heslop, D., Roberts, A.P., Rey, D. & Mohamed, K.J., 2016. Discrimination of biogenic and detrital magnetite through a double Verwey transition temperature, *J. geophys. Res.,* **121**(1), 3–14.

Church, N., Feinberg, J. & Harrison, R., 2011. Low-temperature domain wall pinning in titanomagnetite: quantitative modeling of multidomain first-order reversal curve diagrams and AC susceptibility, *Geochem. Geophys. Geosyst.,* **12**(Q07Z27), doi: 10.1029/2011GC003538.

Coe, R.S., Egli, R., Gilder, S.A. & Wright, J.P., 2012. The thermodynamic effect of nonhydrostatic stress on the Verwey transition, *Earth planet. Sci. Lett.,* **319–320,** 207–217.

Coker, V.S. *et al.*, 2007. Cation site occupancy of biogenic magnetite compared to polygenic ferrite spinels determined by X-ray magnetic circular dichroism, *Eur. J. Mineral.,* **19**(5), 707–716.

Dunlop, D.J., 2006. Inverse thermoremanent magnetization, *J. geophys. Res.,* **111**(B12S02), doi:10.1029/2006JB004572.

Dunlop, D.J. & Ozdemir, O., 2018. Remanence cycling of 0.6–135 μm magnetites across the Verwey transition, *Earth Planets Space,* **70,** 164, doi: 10.1186/s40623-018-0928-z.

Engelmann, R., Kontny, A. & Lattard, D., 2010. Low-temperature magnetism of synthetic Fe-Ti oxide assemblages, *J. geophys. Res.,* **115**(B12), B12107, doi: 10.1029/2010jb000865.

Evans, M.E. & Heller, F., 2003. *Environmental Magnetism: Principles and Applications of Environmagnetics,* Academic Press.

Fabian, K. & Shcherbabov, V.P., 2020. The magnetization of the ocean floor: stress and fracturing of titanomagnetite particles by low-temperature oxidation, *Geophys. J. Int.,* **221,** 2104–2112.

Frankel, R.B., Papaefthymiou, G.C., Blakemore, R.P. & O'Brien, W., 1983. Fe_3O_4 precipitation in magnetotactic bacteria, *Biochim. Biophys. Acta,* **763,** 147–159.

Frankland, B.W. & Zumbo, BD., 2002. Quantifying bimodality Part I: an easily implemented method using SPSS, *J. Mod. Appl. Stat. Methods,* **1**(1), 22. DOI: 10.22237/jmasm/1020255780.

Frankland, B.W. & Zumbo, BD., 2009. Quantifying bimodality Part 2: a likelihood ratio test for the comparison of a unimodal normal distribution and a bimodal mixture of two normal distributions, *J. Mod. Appl. Stat. Methods,* **8**(1), 5. doi: 10.22237/jmasm/1241136240.

Gallagher, K.J., Feitknecht, W. & Mannweiler, U., 1968. Mechanism of oxidation of magnetite to γ-Fe_2O_3, *Nature,* **217**(5134), 1118–1121.

Gattacceca, J., Rochette, P., Lagroix, F., Mathé, P.E. & Zanda, B., 2011. Low temperature magnetic transition of chromite in ordinary chondrites, *Geophys. Res. Lett.,* **38**(10), L10203, doi: 10.1029/2011gl047173.

Hodych, J.P., Mackay, R.I. & English, G.M., 1998. Low-temperature demagnetization of saturation remanence in magnetite-bearing dolerites of high coercivity, *Geophys. J. Int.,* **132**(2), 401–411.

Honig, J.M., 1995. Analysis of the Verwey transition in magnetite, *J. Alloys Compd.,* **229,** 24–39.

Jackson, P.R., Tucker, G.T. & Woods, H.F., 1989. Testing for bimodality in frequency distributions of data suggesting polymorphisms of drug metabolism-hypothesis testing, *Br. J. Clin. Pharmacol.,* **28,** 655–662.

Kakol, Z., 1990. Magnetic and transport properties of magnetite in the vicinity of the Verwey transition, *J. Solid State Chem.,* **88**(1), 104–114.

Kakol, Z. & Kozlowski, A., 2000. Possible influence of electron—lattice interactions on the Verwey transition in magnetite, *Solid State Sci.,* **2**(8), 737–746.

Kakol, Z., Sabol, J. & Honig, J.M., 1991. Magnetic anisotropy of titanomagnetites $Fe_{3-x}Ti_xO_4$, $0<=x<=0.55$, *Phys. Rev. B,* **44,** 2198–2204.

Kakol, Z. *et al.*, 2012. The effect of doping on global lattice properties of magnetite Fe3-xMexO4 (Me = Zn, Ti and Al), *J. Solid State Chem.,* **192,** 120–126.

Kasama, T., Church, N., Feinberg, J.M., Dunin-Borkowski, R.E. & Harrison, R.J., 2010. Direct observation of ferrimagnetic/ferroelastic domain interactions in magnetite below the Verwey transition, *Earth planet. Sci. Lett.,* **297,** 10–17.

Kasama, T., Harrison, R.J., Church, N.S., Nagao, M., Feinberg, J.M. & Dunin-Borkowski, R.E., 2013. Ferrimagnetic/ferroelastic domain interactions in magnetite below the Verwey transition. Part 1: electron holography and lorentz microscopy, *Phase Transiti.,* **86,** doi: 10.1080/01411594.2012.695373.

Klemme, S., O'Neill, H.S.C., Schnelle, W. & Gmelin, E., 2000. The heat capacity of $MgCr_2O_4$, $FeCr_2O_4$, and Cr_2O_3 at low temperatures and derived thermodynamic properties, *Am. Mineral.,* **85**(11–12), 1686–1693.

Kopp, R.E., Nash, C.Z., Kobayashi, A., Weiss, B.P., Bazylinski, D.A. & Kirschvink, J.L., 2006a. Ferromagnetic resonance spectroscopy for assessment of magnetic anisotropy and magnetostatic interactions: a case study of mutant magnetotactic bacteria, *J. geophys. Res.,* **111**(B12), doi:10.1029/2006JB004529.

Kopp, R.E., Weiss, B.P., Maloof, A.C., Vali, H., Nash, C.Z. & Kirschvink, J.L., 2006b. Chains, clumps, and strings: magnetofossil taphonomy with ferromagnetic resonance spectroscopy, *Earth planet. Sci. Lett.,* **247**(1–2), 10–25.

Kosterov, A., 2003. Low-temperature magnetization and AC susceptibility of magnetite: effect of thermomagnetic history, *Geophys. J. Int.,* **154,** 58–71.

Kosterov, A. & Fabian, K., 2008. Twinning control of magnetic properties of multidomain magnetite below the Verwey transition revealed by measurements on individual particles, *Geophys. J. Int.,* **174**(1), 93–106.

Kozlowski, A., Metcalf, P., Kakol, Z. & Honig, J.M., 1996. Electrical and magnetic properties of $Fe_{3-z}Al_zO_4$ ($z<0.06$), *Phys. Rev. B,* **53**(22), 15 113–15 118.

Krasa, D., Muxworthy, A.R. & Williams, W., 2011. Room- and low-temperature magnetic properties of 2-D magnetite particle arrays, *Geophys. J. Int.,* **185,** 167–180.

Lam, K.P. *et al.*, 2010. Characterizing magnetism of individual magnetosomes by X-ray magnetic circular dichroism in a scanning transmission X-ray microscope, *Chem. Geol.,* **270**(1–4), 110–116.

Lee, J., Kwon, S.G., Park, J.-G. & Hyeon, T., 2015. Size dependence of metal–insulator transition in stoichiometric Fe_3O_4 nanocrystals, *Nano Lett.,* **15**(7), 4337–4342.

Li, J.H., Wu, W.F., Liu, Q.S. & Pan, Y.X., 2012. Magnetic anisotropy, magnetostatic interactions and identification of magnetofossils, *Geochem. Geophys. Geosyst.,* **13,** doi:10.1029/2012GC004384.

Liu, Q., Banerjee, S.K., Jackson, M.J., Fahu, C., Yongxin, P. & Rixiang, Z., 2004. Determining the climatic boundary between the Chinese loess and palaeosol: evidence from aeolian coarse-grained magnetite, *Geophys. J. Int.,* **156**(2), 267–274.

Liu, Q.S. & Yu, Y.J., 2004. Multi-cycle low-temperature demagnetization (LTD) of multidomain Fe_3O_4 (magnetite), *J. Magn. Magn. Mater*., **283**(2-3), 150–156.

Liu, Q.S., Roberts, A.P., Larrasoana, J.C., Banerjee, S.K., Guyodo, Y., Tauxe, L. & Oldfield, F., 2012. Environmental magnetism: principles and applications, *Rev. Geophys.,* **50**(Rg4002), doi: 10.1029/2012RG000393.

Longchamp, B.M., 2019. Pseudotachylyte remanence confirms generation along low-angle normal fault planes, 47 pp, *MS thesis*, University of Minnesota, Minneapolis MN.

Maher, B.A. & Thompson, R., 1999. *Quaternary Climates, Environments and Magnetism,* 390pp., Cambridge Univ. Press.

Mang, C. & Kontny, A., 2013. Origin of two Verwey transitions in different generations of magnetite from the Chesapeake Bay impact structure, USA, *J. geophys. Res.,* **118**(10), 5195–5207.

Moskowitz, B.M., Frankel, R. & Bazylinski, D., 1993. Rock magnetic criteria for the detection of biogenic magnetite, *Earth planet. Sci. Lett.,* **120,** 283–300.

Moskowitz, B.M., Jackson, M. & Kissel, C., 1998. Low-temperature magnetic behavior of titanomagnetites, *Earth planet. Sci. Lett.,* **157**(3–4), 141–149.

Moskowitz, B.M., Bazylinski, D.A., Egli, R., Frankel, R.B. & Edwards, K.J., 2008. Magnetic properties of marine magnetotactic bacteria in a seasonally stratified coastal pond (Salt Pond, MA, USA), *Geophys. J. Int.,* **174**(1), 75–92.

Muxworthy, A.R., 1999. Low-temperature susceptibility and hysteresis of magnetite, *Earth planet. Sci. Lett.,* **169**(1-2), 51–58.

Muxworthy, A.R. & McClelland, E., 2000. Review of the low-temperature magnetic properties of magnetite from a rock magnetic perspective, *Geophys. J. Int.,* **140**(1), 101–114.

Özdemir, Ö. & Dunlop, D.J., 1999. Low-temperature properties of a single crystal of magnetite oriented along principal magnetic axes, *Earth planet. Sci. Lett.,* **165**(2), 229–239.

Özdemir, Ö. & Dunlop, D.J., 2010. Hallmarks of maghemitization in low-temperature remanence cycling of partially oxidized magnetite nanoparticles, *J. geophys. Res.,* **115**(B02101), doi:10.1029/2009JB006756.

Özdemir, Ö., Dunlop, D.J. & Moskowitz, B.M., 1993. The effect of oxidation of the Verwey transition in magnetite, *Geophys. Res. Lett.,* **20,** 1671–1674.

Readman, P.W. & O'Reilly, W., 1971. Oxidation processes in titanomagnetites, *Z. Geophys.,* **37,** 329–338.

Reynolds, R.L. *et al.*, 2014a. Iron oxide minerals in dust of the Red Dawn event in eastern Australia, September 2009, *Aeolian Res.,* **15,** 1–13.

Reynolds, R.L. *et al.*, 2014b. Composition of dust deposited to snow cover in the Wasatch Range (Utah, USA): controls on radiative properties of snow cover and comparison to some dust-source sediments, *Aeolian Res.,* **15,** 73–90.

Reynolds, R.L. *et al.*, 2020. Dust deposited on snow cover in the San Juan Mountains, Colorado, 2011–2016: compositional variability bearing on snow-melt effects. *J. geophys. Res.,* **125,** e2019JD032210. https://doi.org/10.1029/2019JD032210.

Rozenberg, G.K., Hearne, G.R., Pasternak, M.P., Metcalf, P.A. & Honig, J.M., 1996. Nature of the Verwey transition in magnetite (Fe3O4) to pressures of 16 GPa, *Phys. Rev. B,* **53**(10), 6482–6487.

Senderov, E., Dogan, A.U. & Navrotsky, A., 1993. Nonstoichiometry of magnetite-ulvospinel solid-solutions quenched from 1300° C, *Am. Mineral.,* **78**(5-6), 565–573.

Shepherd, J.P., Koenitzer, J.W., Aragón, R., Spal/ek, J. & Honig, J.M., 1991. Heat capacity and entropy of nonstoichiometric magnetite ($Fe_{3(1-\delta)}O_4$: The thermodynamic nature of the Verwey transition, *Phys. Rev. B,* **43**(10), 8461–8471.

Smirnov, A.V., 2009. Grain size dependence of low-temperature remanent magnetization in natural and synthetic magnetite: experimental study, *Earth Planets Space,* **61**(1), 119–124.

Smirnov, A.V. & Tarduno, J.A., 2000. Low-temperature magnetic properties of pelagic sediments (Ocean Drilling Program Site 805C): tracers of maghemitization and magnetic mineral reduction, *J. geophys. Res.,* **105**(B7), 16457–16471.

Smirnov, A.V. & Tarduno, J.A., 2011. Development of a low-temperature insert for the measurement of remanent magnetization direction us-

ing superconducting quantum interference device rock magnetometers, *Geochem. Geophys. Geosyst.,* **12**(4), Q04Z23, doi: 10.1029/2011gc003517.

Svindrych, Z., Janu, Z., Kozlowski, A. & Honig, J.M., 2012. Low-temperature magnetic anomaly in magnetite, *Phys. Rev. B,* **86,** 214406, doi.org/10.1103/PhysRevB.86.214406.

van Velzen, A.J. & Dekkers, M.J., 1999. Low-temperature oxidation of magnetite in loess-paleosol sequences: a correction of rock magnetic parameters, *Stud. Geophys. Geod.,* **43**(4), 357–375.

Verwey, E.J., 1939. Electronic conduction of magnetite (Fe_3O_4) and its transition at low temperature, *Nature,* **144,** 327–328.

Walz, F., 2002. The Verwey transition - a topical review, *J. Phys. Condens. Matter,* **14**(12), R285–340.

SUPPORTING INFORMATION

Supplementary data are available at *GJI* online.

Table S1. Verwey transition temperatures from IRM database.
Table S2. Verwey transition temperatures from published sources.
Table S3. Verwey transition temperatures for single crystal magnetite (scm) synthesized at high temperature ($T > 1273$ K) from published sources.

Please note: Oxford University Press are not responsible for the content or functionality of any supporting materials supplied by the authors. Any queries (other than missing material) should be directed to the corresponding author for the PAPER.